doi: 10.17221/17/2015-RAE

Mechanical properties of pellets in compression

Ľ. Kubík[1], V. Kažimírová[2]

[1]*Department of Physics, Faculty of Engineering, Slovak University of Agriculture in Nitra, Nitra, Slovak Republic*

[2]*Department of Production Engineering, Faculty of Engineering, Slovak University of Agriculture in Nitra, Nitra, Slovak Republic*

Abstract

Kubík Ľ., Kažimírová V. (2015): **Mechanical properties of pellets in compression**. Res. Agr. Eng., 61 (Special Issue): S1–S8.

The paper deals with the evaluation of mechanical properties of the cylinder pellet samples. The pellets were made from hay by the granulating machine MGL 200 (Kovonovak) provided by the Department of Production Engineering, Slovak University of Agriculture in Nitra. The pellets were submitted to compressive loading. The compressive loading curves of dependencies of force on strain and force on time were realised by the test stand Andilog Stentor 1000. Certain mechanical parameters were determined, namely the diameter of the sample, length of the sample, force at 10% of strain, force in the first maximum of the force – strain curve, strain in the first maximum of the force – strain curve, modulus of elasticity, force in the inflex point of the force – time and force – strain curves and strain and stress in the inflex point of the force – time and force – strain curves. Significant correlations of the mechanical parameters were observed between the inflex point and the first maximum point of the loading curves. There were find out, the compression force, stress and strain in the inflex point significantly correlate with the force, stress and strain in the first maximum.

Keywords: deformation stress; inflex point; Young's modulus

Plant biomass is available in large quantities, and can be utilized for sustainable heat and power production, when used as fuel (Stelte et al. 2011a). Biodiesel and bioethanol are also new fuels with good thermic properties (Božiková, Hlaváč 2013). But determination of impurities in biofuels is very important (Valach et al. 2013). Vitázek et al. (2013) studied the gravimetric properties of solid biofuels. Agricultural and forest waste as well as industrial products are available materials for biofuel pellet production. By pelletization, raw biomass can be converted into a pellet form with improved fuel quality such as increased bulk density, and uniformed shape and size (Liu et al. 2014). However, the use of different raw materials may have opposite effects on the final densified product. Pellet quality is usually measured by means of bulk density and pellet durability. Mechanical durability is a parameter that is defined by the Technical Specification CEN/TS 14588:2003 as the ability of densified biofuels to remain intact when handled, whereas durability refers to the amount of fines that are recovered from pellets after these have been subjected to mechanical or pneumatic agitation (Gil et al. 2010). The mechanical strength of the pellets is affected by many factors, including compression force and temperature, particle size, and chemical composition of biomass feedstocks (Kaliyan, Morey 2009). Wood pellets are a clean and convenient fuel. They are mostly produced from sawdust, wood chips and wood shavings. Combustion of straw pellets releases smaller amounts of particulates, sulfur,

Supported by the European Community, Project No. 26220220180, and Scientific Grant Agency of the Ministry of Education of Slovak Republic and the Slovak Academy of Sciences – VEGA, Grant No. 1/085400/14.

doi: 10.17221/17/2015-RAE

carbon monoxide, arsenic, carbon dioxide and other greenhouse gases than straw used as fuel. This is also true for wood pellet and wood combustion. However, high ash, nitrogen and chlorine content cause noxious and corrosive emissions for straw as well as straw pellets (Sultana, Kumar 2012). Biomass from plants is a cellular material of high porosity, as the plant cells' interior consists mainly of a large vacuole filled with water, or air in case of dried biomass. The plant cell wall is a composite material consisting of the amorphous polymer lignin, hemicelluloses and partially crystalline cellulose as reinforcement. In addition, minor amounts of extraneous materials can be found. Pellet strength as well as fracture surface analysis provide insight into the level and type of internal bonding. Breaking the pellets using the low speed in the compression test and the higher speed of breaking the pellet manually may have different mechanisms of failure since the polymers show viscoelastic behavior (Stelte et al. 2011b). Newton et al. (1971) evaluated the tensile strength of the pellets though the diametral compression test. Biomass quality concerns have hindered the development of grass biomass for residential combustion, with no comprehensive evaluation system for grass pellet quality. Quality labeling will strengthen the fledgling grass biomass heating market, gain consumer confidence, and help to control combustion related emissions. The proposed system sums qualitatively different parameters into one Quality Index for relative evaluation and ranking of grass pellets for residential combustion potential (Cherney, Verma 2013).

Hroncová and Ladomerský (2014) studied pellets which were made using the straw and hay. The pellets were prepared by mixing plant residues with spruce shavings as well as from pure materials, i.e. wheat straw, hay and sawdust. Individual types of biomass were mixed in various ratios: 50% wheat straw + 50% hay, 50% wheat straw + 50% sawdust, 50% hay + 50% sawdust, 33% wheat straw + 33% hay + 33% sawdust. Pilz et al. (2013) illustrated how and to which extent available know-how can be applied to fuel production from hay. The adaption of selected parameters led to fuel pellets with good physical-mechanical properties. However, during combustion tests in a dedicated pellet boiler high emissions above required emission thresholds have been measured.

The objective of this study was to investigate the effects of the compression force on the pellets and determine the mechanical parameters at the loading. The next objective was determination of the compressive strain in the first maximum of the compressive curves. The initial firmness of the pellets was determined as the force at the 10% of the compressive strain on the loading curve. The next parameter of the firmness was the force in the inflex point of the compression curve at the corresponding compressive strain. The third parameter of the firmness of the pellets was the force at the first maximum at the compressive strain on the loading curve. The last objective was determination of Young's modulus of elasticity by means of two different methods.

MATERIAL AND METHODS

Hay was producted by drying of hair grass (*Agrostis tenius*), cocksfoot grass (*Dactylis glomerata*) and meadow fescue (*Festuca pratensis*) plants. Plants were harvested in June 2013 in the Nitra region, Slovak Republic. Varieties of grasses were represented in the same percentage rate in the hay. Hay contained 28–38% of rough fibrous material and was consisted from plant leafs and stems. The pellets were made from hay by the granulating machine MGL 200 (Kovo Novák, Cotonice, Czech Republic) on the Department of Production Engineering, Slovak University of Agriculture in Nitra. The granulating machine was furnished with the press equipment with disc pelletizer. In the production of the hay pellets no binding agent was used except for watter. Heat value of the hay was 16 720 kJ/kg, the moisture of pellets was 9.3% and density of pellets was 2,265 kg/m^3 (Kažimírová et al. 2013). The pellets were submitted to the compressive loading. The strength of the pellets was evaluated via the quasi static compression test, which was used to study the compaction behavior of tomatoes by Blahovec et al. (1988). The result of the single test is the loading curve, which is dependence between compress force F (N) and compressive strain ε (mm/mm) of the pellet. The base for the determination of compressive strain is the initial dimension of the pellet, which corresponds with its length l_0. The inflex point (F_{inf}, ε_{inf}) was determined on the compression curve. It is the point on the curve between the beginning and the first maximum (F_m, ε_m), which has the following properties: the slope of the dependence F(ε) is decreasing in this point; the slope of the curve is non increasing in any point of the interval (ε_{inf}, ε_m); neither point

doi: 10.17221/17/2015-RAE

of the interval (0, ε_{inf}) has not the properties – the first maximum of dependence (F_m, ε_m) is indicated as the first local maximum of the dependence $F(\varepsilon)$, after which F is decreasing at least at 10%. The cubic regression equations of the dependence $F(\varepsilon)$ were evaluated on the intervals (0, F_m):

$$F = a\varepsilon^3 + b\varepsilon^2 + c\varepsilon + d \quad (1)$$

where:
F – compressive force (N)
ε – compressive strain (mm/mm)
a – regression coefficient (N/mm/mm^3)
b – regression coefficient (N/mm/mm^2)
c – regression coefficient (N/mm/mm)
d – regression coefficient (N)

The cubic regression equations were evaluated also on the intervals (0, F_m) and the inflex points were determined for the dependencies of force F (N) on time t (s):

$$F = et^3 + ft^2 + gt + h \quad (2)$$

where:
F – compressive force (N)
t – time of compression (s)
e – regression coefficient (N/s^3)
f – regression coefficient (N/s^2)
g – regression coefficient (N/s)
h – regression coefficient (N)

The times t_{inf} (s) and forces F_{inf} (N) were determined in the inflex points on the curves $F(t)$. Compressive strains ε_{inf} (mm/mm) and compressive stresses σ_{inf} (MPa) in the inflex point of the loading curves and compressive strains ε_m (mm/mm) and stresses σ_m (MPa) in the first maximum of the loading curves were also enumerated.

The initial firmness of the pellets was determined as the force F_{10} (N) at the 10% of the compressive strain on the loading curve. The second parameter of the firmness was the force F_{inf} (N) in the inflex point of the compression curve at the compressive strain ε_{inf} (mm/mm). The third parameter of the firmness of the pellets was the force F_m at the first maximum at the ε_m compressive strain on the loading curve.

The cylindrical pellets were compressed between a lower steel plate and an upper steel circular plate in the longitudinal direction. The upper plate, attached to the Andilog Stentor 1000 test stand (Andilog Technologies, Vitrolles, France), compressed the cylinder at a speed of 10 mm/min until failure was observed. The compression curves were determined as the dependences of the force F (N) on the strain ε (mm/mm) and the dependences of the force F (N) on time t (s). Time of the compression was calculated from the speed of the test stand 10 mm/min and the elongation Δl (mm) also measured by the stand. The several mechanical parameters of the pellets were enumerated on the basis of the dependence of force on time and strain and on the basis of the inflex points of the loading curves (Blahovec et al. 1988). The compressive strain in the first maximum of the compressive curves was enumerated from the equation:

$$\varepsilon_m = \frac{\nu t_m}{l_0} \quad (3)$$

where:
ε_m – compressive strain in the first maximum of the loading curve $F(\varepsilon)$ (mm/mm)
ν – speed of deformation (mm/min)
t_m – time in the first maximum (min)
l_0 – original length of the sample (mm)

Time t_m (s) was determined in the first maximum of the compression loading curves of the dependence of force F (N) on time t (s). The compressive strains ε_{mp} (mm/mm) were also evaluated from the first maximum of the compression loading curves of the dependence of force F (N) on the strain ε (mm/mm).

The compressive strain in the inflex point of the compressive curves was enumerated from the equation:

$$\varepsilon_{inf} = \frac{\nu t_{inf}}{l_0} \quad (4)$$

where:
ε_{inf} – compressive strain in the inflex point of the loading curve $F(\varepsilon)$ (mm/mm)
ν – speed of deformation (mm/min)
t_{inf} – time in the inflex point (min)
l_0 – original length of the sample (mm)

The compressive stress in the first maximum of the loading curves was enumerated from the equation:

$$\sigma_m = \frac{4F_m}{\pi d^2}(1 - \varepsilon_m) \quad (5)$$

where:
σ_m – compressive stress in the first maximum of the loading curve $\sigma(\varepsilon)$ (MPa)

doi: 10.17221/17/2015-RAE

ε_m – compressive strain in the first maximum of the loading curve F(ε) (mm/mm)
F_m – force in the first maximum of the loading curve $F(\varepsilon)$ (N)
d – original diameter of the sample (mm)

The compressive stresses σ_{mp} (MPa) were also evaluated from the first maximum of the compression loading curves of the dependence of force F (N) on the strain e (mm/mm).

The compressive stress in the inflex point of the loading curves was enumerated from the equation:

$$\sigma_{inf} = \frac{4F_{inf}}{\pi d^2}(1 - \varepsilon_{inf}) \quad (6)$$

where:
σ_{inf} – compressive stress in the inflex point of the loading curve σ(ε) (MPa)
ε_{inf} – compressive strain in the inflex point of the loading curve $F(\varepsilon)$ (mm/mm)
F_m – force in the inflex point of the loading curve $F(\varepsilon)$ (N)
d – original diameter of the sample (mm)

The Young's modulus of elasticity was calculated from the equation:

$$E = \frac{4\Delta F l_0}{\nu \Delta t \pi d^2} \quad (7)$$

where:
E – Young's modulus of elasticity (MPa)
$\Delta F/\Delta t$ – the slope of the loading curve F(t) (N/s)
ν – speed of deformation (mm/s)
l_0 – original height of the sample (mm)
d – original diameter of the sample (mm)

Young's modulus of elasticity E_e (MPa) was also evaluated as the slope of the linear part of dependences of stress σ (MPa) on the strain e (mm/mm). The regression equations were determined as:

$$\sigma = E_e \varepsilon + m \quad (8)$$

where:
σ – compressive stress (MPa)
ε – compressive strain (mm/mm)
E_e – regression coefficient –Young's modulus of elasticity (MPa)
m – regression coefficient (MPa)

RESULTS AND DISCUSSION

Compression diagrams of the cylinder pellet samples as dependence of force F (N) on strain e (mm/mm) are presented in Fig. 1. Dependencies were fitted by the cubic regression equations (1). Regression coefficients of the cubic regression equations (1) are presented in Table 1. The loading curves of different pellets had similar development, but the line shapes were different. There were influenced by the different lengths of the pellet samples. Compression diagrams of the cylinder pellet samples as dependence of force F (N) on time t (s) are presented in Fig. 2. Dependencies were fitted by the cubic regression equations (2). Regression coefficients of the cubic regression equations (2) are presented in Table 1. The shape lines of the dependencies $F(t)$ were very similar to the shape lines of dependencies $F(\varepsilon)$ presented in Fig. 1. The time of the compression was calculated from the speed of the test stand (10 mm/min)

Table 1. Regression coefficients of the cubic regression equations (1) of the dependence of force F (N) on strain ε (mm/mm) according to Fig. 1 and Eq. (2) of the dependence of force F (N) on time t (s) according to Fig. 2

n	d (mm)	l_0 (mm)	Dependence of force on strain: a (N/mm/mm^3)	b (N/mm/mm^2)	c (N/mm/mm)	d (N)	R^2	Dependence of force on time: e (N/s^3)	f (N/s^2)	g (N/s)	h (N)	R^2
1	6.45	10.45	–18289.0000	2535.8000	83.8200	0.7170	0.9974	–0.0795	0.6910	1.2346	0.7609	0.9969
2	6.20	9.30	–3120.0000	1621.7000	–23.0890	0.6783	0.9997	–0.0180	0.5208	–0.4138	0.6783	0.9997
3	6.25	10.30	483.2400	–147.9800	80.1050	1.0516	0.9755	–0.0004	0.0120	1.1669	0.2235	0.9899
4	6.25	14.45	263.0600	445.7600	83.2070	2.0077	0.9983	–0.0027	0.1763	–0.3234	5.8662	0.9964
5	6.30	7.50	–3368.4000	1891.9000	–125.2100	2.5120	0.9979	–0.0370	0.9343	–2.7824	2.5120	0.9979
6	6.30	9.60	–5709.7000	764.5700	130.8100	3.2790	0.9920	–0.0419	0.3576	1.7553	5.6569	0.9939
7	6.20	12.95	13607.0000	-5534.0000	727.4300	6.3380	0.9922	0.0571	–1.2967	10.7020	5.3773	0.9961

d – original diameter of the sample; l_0 – original length of the sample; a, b, c, d – regression coefficients of Eq. (1); e, f, g, h – regression coefficients of Eq. (2); R^2 – coefficient of determination; n – number of sample

doi: 10.17221/17/2015-RAE

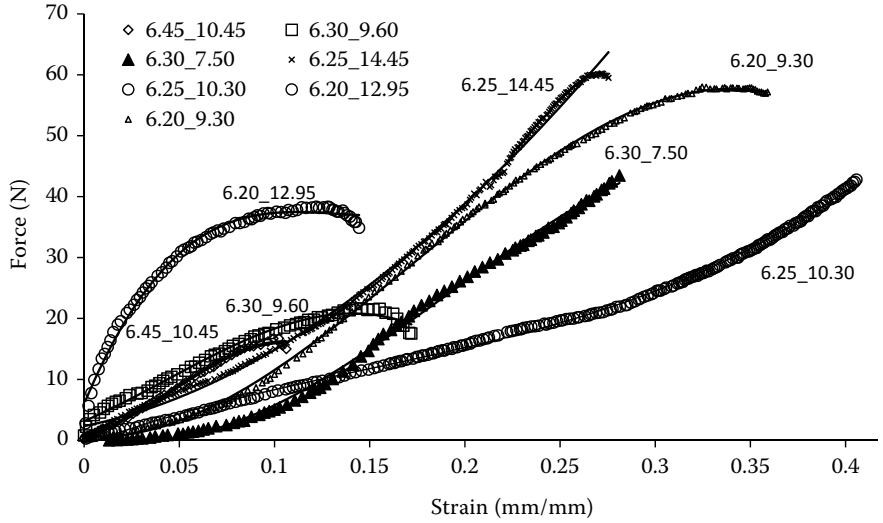

Fig. 1. Compression diagrams of the cylinder pellet samples as a dependence of force F (N) on strain ε (mm/mm). Diameters d (mm) of the pellets are presented in the first column of the legend and lengths l_0 (mm) in the second column

and the elongation Δl (mm) measured by the test stand. The continual proportions were created among dependencies $F(\varepsilon)$ in Fig. 1 and $F(t)$ in Fig. 2.

The moduli of elasticity of the pellet samples were determined in two ways. The example of the first method – determination from the slope of the linear part of the dependency of stress on strain is presented in Fig. 3. The results are presented in Table 2. The second method was calculation from the Eq. (7). Mechanical properties of the cylinder pellet samples after compression are presented in Table 3.

The quantities determined in the compression test of the pellets were correlated. These are confirmed mathematically by the matrix of the correlation coefficients in Table 4. The high absolute values of the correlation coefficients were obtained for the pairs: $F_m - \sigma_m$, $F_{inf} - \sigma_{inf}$, $F_m - \sigma_{mp}$, $\sigma_m - \sigma_{mp}$, $\varepsilon_m - \varepsilon_{mp}$, $\varepsilon_m - \varepsilon_{inf}$ and $E - E_e$. The quantities in the pairs are proportional for following pairs: $F_m - \sigma_m$, $F_{inf} - \sigma_{inf}$, $F_m - \sigma_{mp}$. There are the quantities in the same points of the compressive loading curves. The pairs of quantities $\sigma_m - \sigma_{mp}$, $\varepsilon_m - \varepsilon_{mp}$ and $E - E_e$ represents the same quantities obtained by different ways. The pair $\varepsilon_m - \varepsilon_{inf}$ is interesting because it represents significant relation between inflex points and first maximum points of the compressive loading curves. The significant values (but lower than previous) of the correlation coefficients were also obtained for the pairs: $F_{inf} - \sigma_m$, $F_{inf} - \sigma_{inf}$, $F_{inf} - \sigma_{mp}$, $\sigma_{inf} - \sigma_{mp}$, $\sigma_{inf} - \sigma_m$; confirming the relation between inflex points and first maximum points of the compressive loading curves. According to Table 4, the firmness of the pellet samples depends mainly on the coordinates F_m, σ_m, σ_{mp}, ε_m and ε_{mp} of the first maximum of the compression loading curves $F(\varepsilon)$, $\sigma(\varepsilon)$ and $F(t)$ and also on the coordinates F_{inf}, σ_{inf} and ε_{inf} of the inflex point of the compression loading curves $F(\varepsilon)$, $\sigma(\varepsilon)$ and $F(t)$. The initial firmness of the pellets determined by the force F_{10} at 10% deformation at strain 0.1 mm/mm did not influence on the total firmness of the pellet samples. This means that the value of the strain in

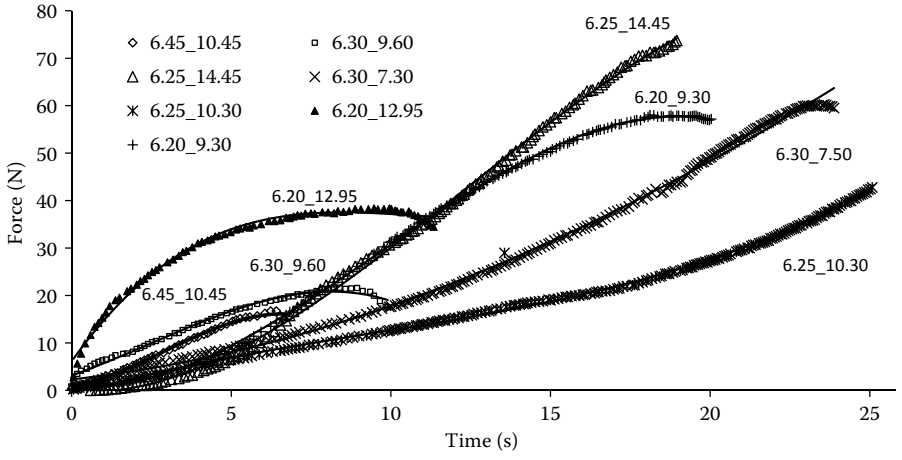

Fig. 2. Compression diagrams of the cylinder pellet samples as a dependence of force F (N) on time t (s). Diameters d (mm) of the pellets are presented in the first column of the legend and lengths l_0 (mm) in the second column

doi: 10.17221/17/2015-RAE

Table 2. Determination of Young's modulus of elasticity E_e by means of slope of linear dependence σ(ε). Regression coefficients of the linear regression equations (8) of the dependence of stress σ (MPa) on strain ε (mm/mm) according to Fig. 3

n	d (mm)	l_0 (mm)	E_e (MPa)	m (MPa)	R^2
1	6.45	10.45	5.2973	0.0045	0.9963
2	6.20	9.30	8.1642	–0.4472	0.9982
3	6.25	10.30	2.5786	–0.0035	0.9982
4	6.25	14.45	7.7954	–0.3348	0.9938
5	6.30	7.50	7.4877	–0.6330	0.9949
6	6.30	9.60	4.3809	0.1326	0.9915
7	6.20	12.95	7.0290	0.6116	0.9385

d – original diameter of the sample; l_0 – original length of the sample; E_e – modulus of elasticity; m – regression coefficients of Eq. (8); R^2 – coefficient of determination; n – number of sample

the interval (ε_{inf}, ε_m) more influenced on the firmness of the pellet sample than initial firmness given by the strain interval (0, 0.10). Influence of the diameter d of the pellets on the total firmness was lower than the influence of parameters in the inflex points and in the first maximum, but higher than was the influence of the length l_0.

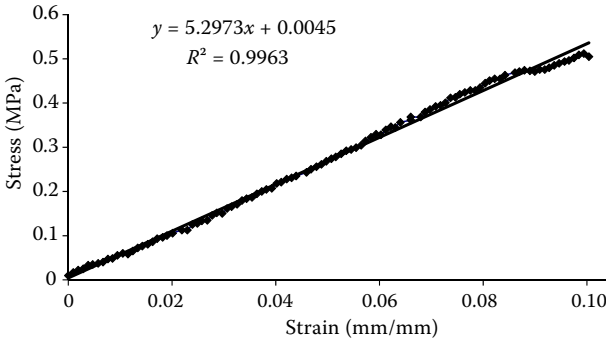

Fig. 3. Determination of modulus of elasticity of the cylinder pellet sample of diameter 6.45 mm and length 10.45 mm as the slope of the linear part of dependence of stress (MPa) on strain (mm/mm). Determined modulus of elasticity E_e = 5.2973 MPa

The values of the mechanical properties of the pellet samples are characterized by high variation because only seven samples of the pellets were used. This means that the standard deviations of the evaluated parameters varied from 0.48% to 23.47%. The average values of the modulus of elasticity ranged from 5.39 MPa to 6.10 MPa. Liu et al. (2014) present the values of the tensile strength of the pellets in the range from 1.51 MPa to 7.10 MPa. Mania et al. (2006) present the values of modulus of elasticity in the range from 0.92 MPa to 1.33 MPa.

Table 3. Mechanical properties of the cylinder pellet samples after compression

n	d (mm)	l_0 (mm)	F_{10} (N)	F_m (N)	ε_{mp} (mm/mm)	σ_{mp} (MPa)	ε_m (mm/mm)	σ_m (MPa)	E_e (MPa)	E (MPa)	F_{inf} (N)	ε_{inf} (mm/mm)	σ_{inf} (MPa)
1	6.45	10.45	16.49	16.69	0.10	0.51	0.10	0.46	5.29	5.05	7.50	0.05	0.22
2	6.20	9.30	10.81	57.91	0.33	1.99	0.33	1.29	8.16	7.86	28.52	0.17	0.78
3	6.25	10.30	7.99	18.08	0.24	0.62	0.29	0.57	2.58	2.57	12.58	0.16	0.34
4	6.25	14.45	14.99	59.90	0.27	1.96	0.34	1.24	7.80	5.99	41.70	0.21	1.07
5	6.30	7.50	5.04	57.46	0.33	1.24	0.34	1.24	7.49	6.90	23.98	0.19	0.64
6	6.30	9.60	17.99	21.62	0.15	0.70	0.15	0.59	4.38	2.37	11.63	0.05	0.35
7	6.20	12.95	37.44	38.34	0.13	1.27	0.12	1.12	7.03	7.03	37.34	0.10	1.12
Average	6.28	10.65	15.82	38.57	0.22	1.18	0.24	0.93	6.10	5.39	23.32	0.13	0.65
s	0.03	0.82	3.71	6.96	0.03	0.21	0.04	0.13	0.73	0.76	4.66	0.02	0.13
s (%)	0.48	7.68	23.47	18.04	15.07	18.14	15.81	13.97	11.92	14.16	19.98	17.82	19.54

d – original diameter of the sample; l_0 – original length of the sample; F_{10} – force at 10% of the strain; F_m – force in the first maximum of the force – strain curve; ε_{mp} – strain in the first maximum determined from the force – strain curve; σ_{mp} – stress in the first maximum determined from the force – strain curve; ε_m – strain in the first maximum of the force – strain curve determined from Eq. (3); σ_m – stress in the first maximum of the force – strain curve determined from Eq. (5); E_e – modulus of elasticity determined from the slope of the linear part of the stress – strain curves; E – modulus of elasticity determined from Eq. (7); F_{inf} – force in the inflex point determined from the force – time curve; ε_{inf} – strain in the inflex point determined from Eq. (4); σ_{inf} – stress in the inflex point determined from Eq. (6); n – number of sample; s – standard deviation

doi: 10.17221/17/2015-RAE

Table 4. Correlation coefficients for the quantities evaluated in the compression test (only correlation coefficients with the absolute value higher than 0.5 are given)

	d	l_0	F_{10}	F_m	ε_{mp}	σ_{mp}	ε_m	σ_m	E_e	E	F_{inf}	ε_{inf}	σ_{inf}
d	1												
l_0		1											
F_{10}		0.589	1										
F_m	–0.511			1									
ε_{mp}			–0.691	0.762	1								
σ_{mp}	–0.635			0.923	0.644	1							
ε_m			–0.701	0.702	0.962	0.619	1						
σ_m	–0.644			0.970	0.682	0.915	0.608	1					
E_e				0.891		0.847		0.887	1				
E				0.788		0.742		0.834	0.923	1			
F_{inf}	–0.681	0.601		0.797		0.856		0.867	0.762	0.681	1		
ε_{inf}				0.770	0.884	0.706	0.949	0.721			0.598	1	
σ_{inf}	–0.704	0.604		0.741		0.811		0.840	0.741	0.682	0.991	0.508	1

d – original diameter of the sample; l_0 – original length of the sample; F_{10} – force at 10% of the strain; F_m – force in the first maximum of the force – strain curve; ε_{mp} – strain in the first maximum determined from the force – strain curve; σ_{mp} – stress in the first maximum determined from the force – strain curve; ε_m – strain in the first maximum of the force – strain curve determined from Eq. (3); σ_m – stress in the first maximum of the force – strain curve determined from Eq. (5); E_e – modulus of elasticity determined from the slope of the linear part of the stress – strain curves; E – modulus of elasticity determined from Eq. (7); F_{inf} – force in the inflex point determined from the force – time curve; ε_{inf} – strain in the inflex point determined from Eq. (4); σ_{inf} – stress in the inflex point determined from Eq. (6)

CONCLUSION

On the basis of Blahovec et al. (1988) work the characteristic point on the loading compressive curve in the compressing of the pellets between two metal plates was determined. It is inflex point between the beginning of the loading curve and its first maximum. Compression force, stress and strain in the inflex point significantly correlating with the force, stress and strain in the first maximum were obtained. Measured values of mechanical parameters of the hay pellets are characterized by high dispersion. Two groups of mechanical parameters characterized by positive and negative values of correlation coefficients were obtained. Diameter of the pellets and the initial firmness had negative correlation coefficients and their connection and influence on the next mechanical parameters were opposite. The initial firmness of the pellets determined by force at 10% deformation at strain 0.1 mm/mm did not influence on the total firmness of the pellet samples.

References

Blahovec J., Houška M., Pokorný D., Patočka K., Kubešová A., Bareš J. (1988): Mechanical properties of tomato fruits and their determination. Research in Agriculture Engineering, 34: 739–751.

Božiková M., Hlaváč P. (2013): Thermal conductivity and thermal diffusivity of biodiesel and bioethanol samples. Acta Technologica Agriculturae, 16: 88–92.

Cherney J.H., Verma V.K. (2013): Grass pellet Quality Index: A tool to evaluate suitability of grass pellets for small scale combustion systems, Applied Energy, 103: 679–684.

Gil M.V., Oulego P., Casal M.D., Pevida C., Pis J.J., Rubiera F. (2010): Mechanical durability and combustion characteristics of pellets from biomass blends. Bioresource Technology, 101: 8859–8867.

Hroncová E., Ladomerský J. (2014): The environmental and energy potential of incinerating various biomass mixtures. Advanced Materials Research, 1001: 114–117.

Kažimírová V., Brestovič T., Opáth R. (2013): Selected properties of agricultural biomass. Research in Agricultural Engineering, 59 (Special Issue): S60–S64.

doi: 10.17221/17/2015-RAE

Kaliyan N., Morey R.V. (2009): Factors affecting strength and durability of densified biomass products. Biomass and bioenergy, 33: 337–359.

Liu Z, Quek A, Balasubramanian R. (2014): Preparation and characterization of fuel pellets from woody biomass, agro-residues and their corresponding hydrochars. Applied Energy, 113: 1315–1322.

Mania S., Tabilb G.L., Sokhansanj S. (2006): Effects of compressive force, particle size and moisture content on mechanical properties of biomass pellets from grasses. Biomass and Bioenergy, 30: 648–654.

Newton J.M., Rowley G., Fell J.T., Peacock D.G., Ridgway, K. (1971): Computer analysis of the relation between tablet strength and compaction pressure. Journal of Pharmacy and Pharmacology, 23: 195–201.

Pilz A., Döhling F., Kirsten C., Weller N., Zeng T. (2013): Pelletizing and energy related use of hay from landscape preservation. Landtechnik, 68: 349–352.

Stelte W., Holm J.K., Sanadi A.R., Barsberg S., Ahrenfeldt J. (2011a): A study of bonding and failure mechanisms in fuel pellets from different biomass resources. Biomass and Bioenergy, 35: 910–918.

Stelte W., Holm J.K., Sanadi A.R., Barsberg S., Ahrenfeldt J. Henriksen U.B. (2011b): Fuel pellets from biomass: The importance of the pelletizing pressure and its dependency on the processing conditions. Fuel, 90: 3285–3290.

Sultana A., Kumar A. (2012): Ranking of biomass pellets by integration of economic, environmental and technical factors. Biomass and Bioenergy, 39: 344–355.

Tabil L.G., Sokhansanj S. (1996): Bulk properties of alfalfa grind in relation to its compaction characteristics. Applied Engineering in Agriculture, 13: 499–505.

Valach M., Mareček J., Hlaváčová Z., Trávniček P., Glos J. (2013): Determination of impurities in biofuels with using a particle size analyzer. Acta Universitatis Agriculturae et Silviculturae Mendelianae Brunensis, 61: 813–817.

Vitázek I., Andoč P., Vitázková B. (2013): Gravimetric analysis of selected solid biofuels. Konstrujovannija, virobnictvo ta ekspluatacija siľskogospodarskich mašin, 43: 240–245.

Received for publication March 10, 2015
Accepted after corrections August 18, 2015

Corresponding author:

RNDr. Ľubomír Kubík, PhD., Slovak University of Agriculture in Nitra, Faculty of Engineering, Department of Physics, Tr. A. Hlinku 2, 949 76 Nitra, Slovak Republic; e-mail: lubomir.kubik@uniag.sk